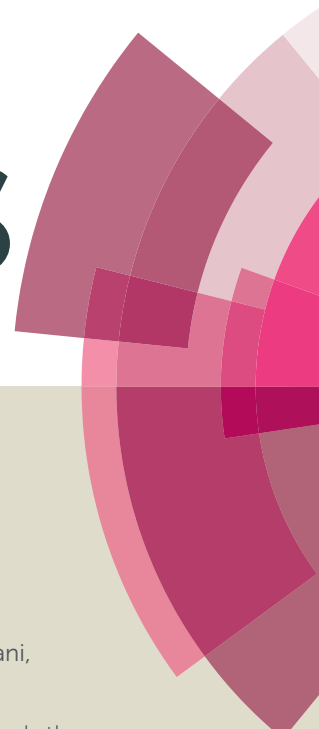


# RSC Advances



This article can be cited before page numbers have been issued, to do this please use: C. Tsai, S. Kamani, C. Yeh, C. Wang, C. Lin, H. Yen, M. Tsai and G. Liou, *RSC Adv.*, 2016, DOI: 10.1039/C6RA18986E.



This is an *Accepted Manuscript*, which has been through the Royal Society of Chemistry peer review process and has been accepted for publication.

*Accepted Manuscripts* are published online shortly after acceptance, before technical editing, formatting and proof reading. Using this free service, authors can make their results available to the community, in citable form, before we publish the edited article. This *Accepted Manuscript* will be replaced by the edited, formatted and paginated article as soon as this is available.

You can find more information about *Accepted Manuscripts* in the [Information for Authors](#).

Please note that technical editing may introduce minor changes to the text and/or graphics, which may alter content. The journal's standard [Terms & Conditions](#) and the [Ethical guidelines](#) still apply. In no event shall the Royal Society of Chemistry be held responsible for any errors or omissions in this *Accepted Manuscript* or any consequences arising from the use of any information it contains.

## Zinc and linkage effects of novel porphyrin-containing polyimides on resistor memory behaviors

Chia-Liang Tsai,<sup>a,†</sup> Kamani Sudhir K Reddy,<sup>b,†</sup> Chen-Yu Yeh,<sup>b,\*</sup> Chin-Li Wang,<sup>c</sup> Ching-Yao Lin,<sup>c,\*</sup> Hung-Ju Yen,<sup>a</sup> Ming-Chi Tsai<sup>a</sup> and Guey-Sheng Liou<sup>a,\*</sup>

Received 00th January 20xx,  
Accepted 00th January 20xx

DOI: 10.1039/x0xx00000x

www.rsc.org/

A new class of porphyrin-containing polyimides, **ZnPor-s-DSDA**, **ZnPor-t-DSDA**, **Por-s-DSDA** and **Por-t-DSDA**, were synthesized from porphyrin-containing diamines and 3,3',4,4'-diphenylsulfone tetracarboxylic dianhydride for resistor-type memory application. The effect of the linkage and zinc metal has been investigated by electrochemistry, molecular simulation, and memory behaviors. The memory devices with different retention time derived from polymers **ZnPor-s-DSDA** (WORM, >3hr) and **ZnPor-t-DSDA** (DRAM, 30s) demonstrated the importance of linkage effect, and the insulate property of polyimides **Por-s-DSDA** and **Por-t-DSDA** also implies the crucial memory behavior by metal chelation.

### INTRODUCTION

Polymers have become the remarkable synthetic materials in these few decades and been applied in novel fields including solar cells,<sup>1</sup> organic thin film transistors (OTFTs),<sup>2</sup> organic light-emitting diodes (OLEDs),<sup>3</sup> electrochromic devices,<sup>4</sup> and memory devices.<sup>5</sup> After the first polymeric memory device was demonstrated by Sliva et al. in 1970,<sup>6</sup> polymer-based memory devices have attracted immense attention and studied for the development of next generation memory device applications, because of their low-cost, three-dimensional stacked structure, organo-processability, and large area fabrication capability.<sup>7</sup> Moreover, there are numerous kinds of polymer materials investigated for memory devices, which generally includes conjugated polymers feature donor-acceptor (D-A) capabilities,<sup>8</sup> non-conjugated polymers bearing side-chain electroactive chromophores,<sup>9</sup> functionalized polyimides (PIs),<sup>10</sup> and polymer hybrids.<sup>11</sup> According to rich structural flexibility of polymeric materials, different types of memory behaviors have been demonstrated, including volatile devices: static random access memory (SRAM) and dynamic random access memory (DRAM); nonvolatile devices: write-once-read-many times (WORM) and rewritable memory (Flash). Among these polymer systems, functional PI was chosen for polymeric memory application due to the excellent combination of advantages: outstanding thermal properties, chemical resistance, and good mechanical properties. In 2006, Kang et al. published the first

PI-based resistor-type memory device, showing a programmable DRAM behavior.<sup>12</sup> Resistive memory device stores data by bi-stable states (high and low conductivities), "1 (ON)" and "0 (OFF)", respectively. Furthermore, the working mechanism of resistor-type memory devices has been studied and divided into charge transfer (CT), filamentary conduction, and space charge trapping. CT is defined as the partial electronic D-A charge transfers. Thus, D-A system based memory devices can easily induce CT result by applying suitable external voltage.<sup>13</sup>

Notably, porphyrin-containing materials were widely used in organic devices, including solar cells,<sup>14</sup> LEDs,<sup>15</sup> and TFTs.<sup>16</sup> Especially, porphyrin derivatives have been demonstrated as good  $\pi$ -bridge moieties owing to its high conjugated, electron-rich, and excellent extinction coefficient, which further make porphyrin-based materials as great candidate for solar-cell applications. In this work, we design three new D-A porphyrin-based PIs, **Por-t-DSDA**, **ZnPor-s-DSDA**, and **Por-s-DSDA**, for resistor-type memory application (Figure 1), which are also compared with **ZnPor-t-DSDA**.<sup>17</sup> In addition, the works published by our lab.<sup>18a,b</sup> both report tunable memory behaviors with various donors and the same acceptor 3,3',4,4'-diphenylsulfone tetracarboxylic dianhydride (DSDA) to compare the electron-donating ability. By further choosing the suitable linkage between the electron donor and acceptor moieties of high performance polymers, tunable memory properties (from insulator to different retention time SRAM) can also be achieved.<sup>18c</sup> Therefore, this D-A PI system consists of electron donor macrocyclic porphyrin derivatives and an excellent acceptor DSDA.<sup>18</sup> The memory behavior of Zn porphyrin-containing PIs (**ZnPor-t-DSDA** and **ZnPor-s-DSDA**) exhibit the DRAM (30 s) and WORM (> 3 hr), respectively, according to different linkage between donor (Zn-porphyrin diamines) and acceptor (DSDA) moieties. However, based on the experimental results, free base porphyrin-containing PIs (**Por-t-DSDA** and **Por-s-DSDA**) did not show any memory behavior under

<sup>a</sup> Institute of Polymer Science and Engineering, National Taiwan University, 1 Roosevelt Road, 4th Sec., Taipei 10617, Taiwan. E-mail: [gqliou@ntu.edu.tw](mailto:gqliou@ntu.edu.tw) (G. S. Liou)

<sup>b</sup> Department of Chemistry and Research Center for Sustainable Energy and Nanotechnology, National Chung Hsing University, Taichung 402, Taiwan. E-mail: [cyyeh@dragon.nchu.edu.tw](mailto:cyyeh@dragon.nchu.edu.tw) (C. Y. Yeh)

<sup>c</sup> Department of Applied Chemistry, National Chi Nan University, Puli, Nantou 54561, Taiwan. E-mail: [cyl@ncnu.edu.tw](mailto:cyl@ncnu.edu.tw) (C. Y. Lin)

<sup>†</sup> These authors contributed equally

Electronic Supplementary Information (ESI) available: Experimental section. Table: basic properties of polyimides. Figure: basic properties of monomers and polyimides.

available applying voltage, indicating that metal zinc is necessary to induce CT by external electric field.



**Figure 1.** Chemical structure of porphyrin-based PIs and memory device.

## RESULTS AND DISCUSSION

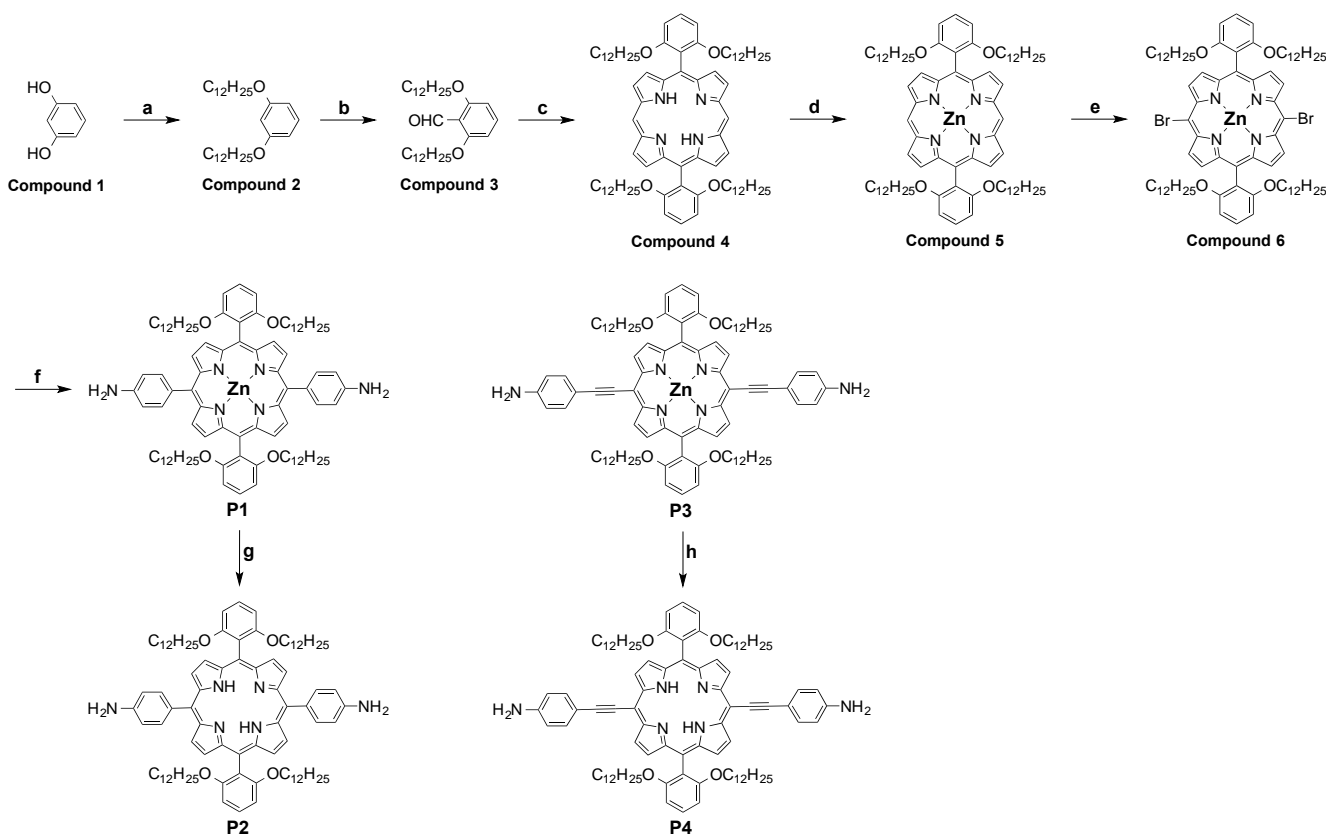
### Monomer Synthesis

The synthetic procedure for diamines **P1-P4** is summarized in [Scheme 1](#) and based on previous strategies.<sup>19</sup> The significant intermediate **compound 6** was prepared with yield >26 % from the Lewis acid (trifluoroacetic acid) catalyzed condensation of **compound 3** and dipyrromethane followed by Zinc-metalation and dibromination. Diamine **P1** was prepared by Pd-catalyzed Sonogashira coupling, which was then used to prepare **P2** by demetalation. Similarly, diamine **P4** was also synthesized by demetalation of **P3**. <sup>1</sup>H NMR, <sup>13</sup>C NMR, elemental analysis, and

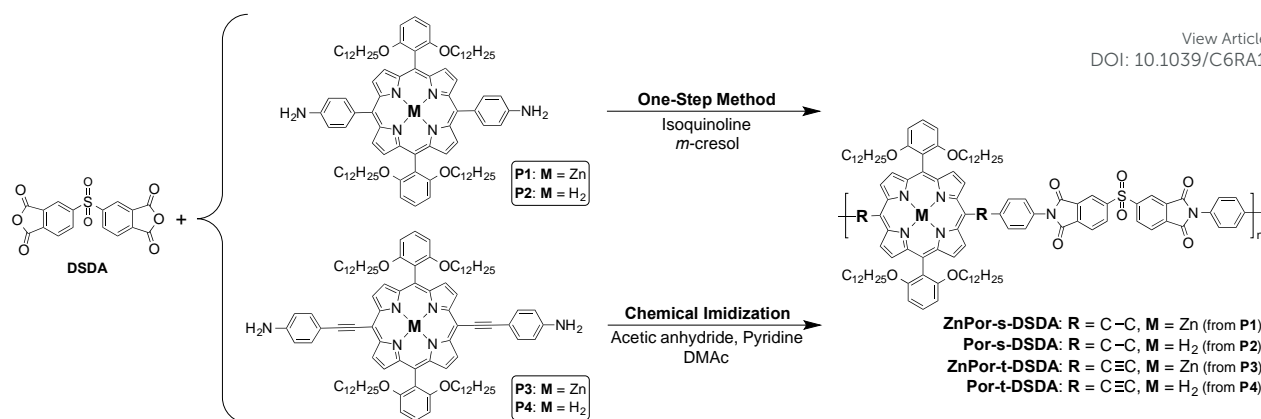
MALDI-TOF MS spectroscopic methods are utilized to characterize the structural information of these new compounds. The bulky alkoxyphenyl long chains were incorporated at the meso-positions to prevent aggregation that can further facilitate the organo-solubility of the prepared porphyrin-based polyimides.

### Basic Properties of Porphyrin-containing PIs

Three novel porphyrin-containing PIs were prepared by the reaction of four different porphyrin diamines (**P1-P4**) and DSDA via a conventional polycondensation reaction as shown in [Scheme 2](#). Porphyrin moiety was introduced as a donor of the PIs in this work because of its planar, electron-rich, highly conjugated, and ease of tuning chemical structure. The inherent viscosity and GPC data of the PIs are listed in [Table S1](#), and the solubility properties examined at 5 wt % are summarized in [Table S2](#). The results exhibited an excellent organo-solubility of these porphyrin-containing PIs due to the long alkoxy chains wrapping and polarity of DSDA. Thus, the good solubility makes these PIs as outstanding memory materials for solvent-casting process. Thermal behaviors of the porphyrin-containing PIs were investigated by TGA and TMA, and the diagrams shown in [Figure S1](#) revealed good thermal property with negligible weight loss up to 330 °C and the glass-transition temperature ( $T_g$ ) in the range of 132-176 °C (as summarized in [Table S3](#)).



**Scheme 1.** Synthetic procedure of diamines **P1-P4**. **Conditions:** **a.** DMSO, 1-bromododecane, KOH, room temperature, 12 h; **b.** 1.6 M *n*-BuLi, DMF; **c.** dipyrromethane, TFA, CH<sub>2</sub>Cl<sub>2</sub>; **d.** Zn(OAc)<sub>2</sub>•4H<sub>2</sub>O, CH<sub>2</sub>Cl<sub>2</sub>, CH<sub>3</sub>OH; **e.** NBS, CH<sub>2</sub>Cl<sub>2</sub>, pyridine, -5 °C to room temperature; **f.** Pd(PPh<sub>3</sub>)<sub>4</sub>, 4-(4,4,5,5-tetramethyl-1,3,2-dioxaborolan-2-yl)aniline, Na<sub>2</sub>CO<sub>3(aq)</sub>, toluene, 100 °C for 5 h; **g.** 16% HCl, CH<sub>2</sub>Cl<sub>2</sub>, room temperature; **h.** 12 M HCl, CH<sub>2</sub>Cl<sub>2</sub>, CH<sub>3</sub>OH, room temperature, Na<sub>2</sub>CO<sub>3(aq)</sub>.



**Scheme 2.** Synthesis and structures of the porphyrin containing polyimides.

### Optical and Electrochemical Properties

The UV-spectra of the porphyrin-containing PIs are depicted in Figure S2, and the energy gap ( $E_g$ ) of the prepared polymers was calculated by the onset wavelength. The electrochemistry was tested by cyclic voltammetry (CV) via casting the PIs onto ITO-coated glass substrates as working electrodes, 0.1 M tetrabutylammonium perchlorate (TBAP) containing dehydrate acetonitrile ( $\text{CH}_3\text{CN}$ ) as electrolyte solution in nitrogen atmosphere. The CV shown in Figure 2 displayed the onset oxidation potentials of the PIs (**ZnPor-t-DSDA**, **Por-t-DSDA**, **ZnPor-s-DSDA**, and **Por-s-DSDA**) to be 0.79, 0.99, 0.75, and 1.00 V, that are related to the highest occupied molecular orbital (HOMO) of 5.23, 5.43, 5.19, and 5.44 eV, respectively, (basis on ferrocene/ferrocenium redox couple which is 4.8 eV below the vacuum level with  $E_{\text{onset}} = 0.36$  V). The results summarized in Table 1 reveal that the HOMO energy levels of the Zn-porphyrin-containing PIs (**ZnPor-t-DSDA** and **ZnPor-s-DSDA**) are higher than those of the corresponding Zn-free PIs, implying Zn-porphyrin with higher electron-donating capability.

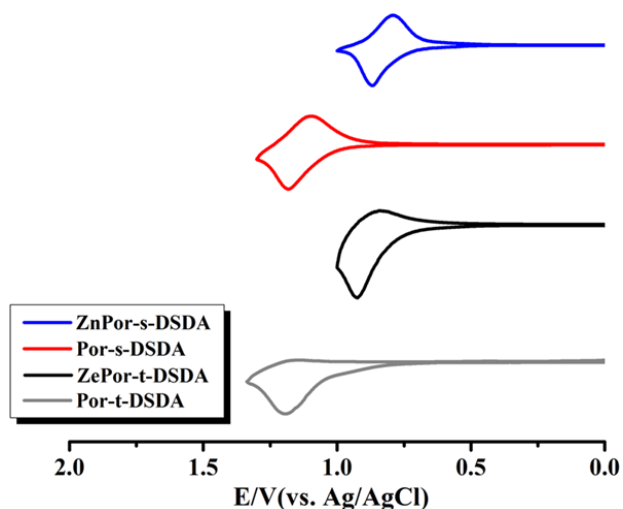


**Figure 2.** CVs of PI films on ITO-coated glass in 0.1 M TBAP/ $\text{CH}_3\text{CN}$  at a scan rate of 50 mV/s.

**Table 1.** Oxidation potentials and energy levels of PIs

Polymer	Oxidation $E_{\text{onset}}$ (V) <sup>a</sup>	$E_g$ (eV) <sup>b</sup>	HOMO (eV) <sup>c</sup>	LUMO (eV) <sup>d</sup>
<b>ZnPor-t-DSDA</b>	0.79	1.78	5.23	3.45
<b>ZnPor-s-DSDA</b>	0.75	1.98	5.19	3.21
<b>Por-t-DSDA</b>	0.99	1.72	5.43	3.71
<b>Por-s-DSDA</b>	1.00	1.86	5.44	3.58

<sup>a</sup> From CVs vs. Ag/AgCl in  $\text{CH}_3\text{CN}$ . <sup>b</sup> The data are calculated from the onset wavelength by the equation:  $E_g = 1240/\lambda_{\text{onset}}$  (energy gap between HOMO and LUMO). <sup>c</sup> The HOMO energy levels were calculated from CV and were referenced to ferrocene (4.8 eV;  $E_{\text{onset}} = 0.36$  V). <sup>d</sup> LUMO energy levels were calculated by the optical method from  $E_g$  and HOMO.

### Memory Device Characteristics

The memory properties of the PIs were characterized by the current-voltage ( $I$ - $V$ ) diagrams of an ITO-coated glass/PI/Al or Au sandwiched device (as shown in Figure 1). The PI film served as an active layer was spin-coated between ITO and Al. A standard thickness of  $\sim 50$  nm was employed to exclude the thickness effect. The  $I$ - $V$  curves of **ZnPor-s-DSDA** depicted in Figure 3(a) and 3(b) show the nonvolatile bi-switching WORM memory property. With the first negative and positive scan from 0 to -6 and 6 V, the device was initially in the OFF state with a current around  $\sim 10^{-12}$  A, then increased sharply from OFF state to  $\sim 10^{-4}$  A (ON state) at threshold voltages of -4.2 V and 4.6 V, respectively. The device derived from **ZnPor-s-DSDA** remained on the ON state in the succeeding negative and positive sweep after turning the power off for long period (>3hr), which is very

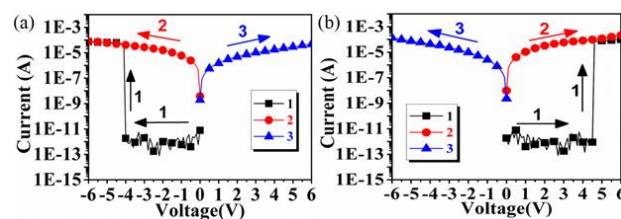


**Figure 3.**  $I$ - $V$  diagrams of the ITO/**ZnPor-s-DSDA**/Al memory devices with the first scan performed (a) negatively and (b) positively.

different to the device of **ZnPor-t-DSDA** manifested as bi-switching DRAM behavior (retention time only 30 s) in our previous study.<sup>17</sup>

Furthermore, the long-term operation at the ON and OFF states of the ITO/**ZnPor-s-DSDA**/Al device with a continuously applied voltage of -1 V was tested and shown in Figure 4. There is negligible degradation in current at both ON and OFF states after 10<sup>4</sup> s under the readout test, indicating an excellent stability of the memory device. While, the devices prepared from **Por-s-DSDA** and **Por-t-DSDA** exhibited no memory property with the corresponding voltage sweeps shown in Figure 5(a) and (b), respectively.

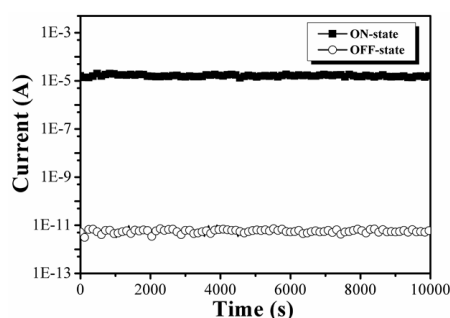


**Figure 4.** Long-term operation at the ON and OFF states of the ITO/**ZnPor-s-DSDA**/Al device with a continuously applied voltage of -1 V for ON and OFF states.

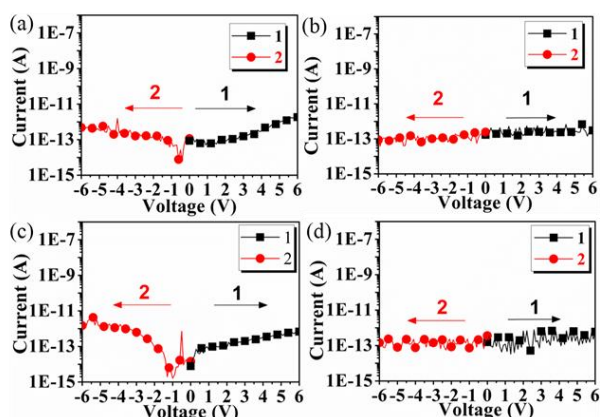


**Figure 5.** I-V diagrams of the ITO/(a) **Por-s-DSDA**, (b) **Por-t-DSDA**/Al memory devices, and ITO/(c) **Por-s-DSDA**, (d) **Por-t-DSDA**/Au memory devices.

### Simulation of Switching Mechanism

To obtain deep insight to the memory performance of porphyrin-based PIs, the molecular simulation is done by using B3LYP/LanL2DZ Gaussian 09 package of the basic unit, and calculated HOMO and LUMO of the prepared PIs are illustrated in Figure 6(a). For electron distribution, the HOMO and LUMO are mainly located at the donor porphyrin moieties and acceptor DSDA, respectively. As the applied external electric field reached the threshold voltage, some electrons localizing at the HOMO transit to the LUMOs, forming a CT formation (ON state). Transit to LUMO5 (**ZnPor-**

**s-DSDA**) and LUMO3 (**ZnPor-t-DSDA**) have more possibility according to the highest overlap of electron distribution between HOMO and LUMO5/3. Meanwhile, other LUMOs in between would possibly accept the electrons excited from HOMO. Thus, the conductive CT complexes were formed by several pathways, including from LUMO5/3 through LUMOs in between then to LUMO or directly be excited from HOMO to LUMO due to intra-/inter- molecular CT. Moreover, the generated electron holes can delocalize to porphyrin moieties, performing an open channel for charge carriers (holes), thus switched the device to ON state. Nevertheless, **Por-s-DSDA** and **Por-t-DSDA**, displaying the similar simulation results as the zinc containing ones, revealed no memory property, confirming the crucial zinc effect on the formation of conductive channels.

According to the simulation results shown in Figure 6(b), the different conformation due to the linkage between porphyrin unit and phenyl ring of **ZnPor-s-DSDA** (single bond) and **ZnPor-t-DSDA** (triple bond) resulted in 65.5° and 0.4°, respectively. The induced electrons localize at DSDA moiety by applying electric field, and the non-coplanar (65.5°) conformational structure of **ZnPor-s-DSDA** becomes a barrier for CT back from DSDA to porphyrin moiety, resulting in much longer retention time (>3hr) than **ZnPor-t-DSDA** (30s). The linkage and non-coplanar effects on memory properties have also been investigated and demonstrated in our previous reports.<sup>20</sup>

It is worth to mention that the memory properties could be induced by both of negative and positive sweeps in the porphyrin PIs with zinc metal. However, the corresponding PIs without zinc did not exhibit any memory behavior. Generally, the holes injection is from ITO (-4.8 eV) to the HOMO of PI in the negative sweep because of the lower band gap between them according to the proposed mechanism for PI memory devices. On the contrary, it is obviously difficult to induce memory behavior when sweep positively as shown in Figure 7(a). However, the devices derived from ITO/**Por-s-DSDA** and **Por-t-DSDA**/Al could not exhibit any memory property even in negative sweep as illustrated in Figure 5(a) and 5(b), indicating that the formation of conductive channel or the holes injection should be difficult for the PIs without zinc metal. Moreover, we also investigated the memory behavior by replacing Al with Au electrode to refer our previous studies<sup>21</sup> in terms of the different work function of metal electrode (Au 5.1 eV and Al 4.2 eV), and the memory property might be easily induced by lower work function of Au electrode. With this in mind, we fabricated the devices of ITO/**Por-s-DSDA**, **Por-t-DSDA**/Au, however, the devices still displayed no memory property neither in negative nor positive sweeps as shown in Figure 5(c) and 5(d), respectively.

According to the experiment results, the occurrence of memory behaviors could be inferred from zinc effect. Figure 7(b) depicts a schematic illustration of the band diagram for the memory device of ITO/Zn-porphyrin-containing PI/Al. The work functions of Zn, ITO, and Al are very close (4.3, 4.8 and 4.2 eV, respectively). Thus, when the external electric

field (negative or positive) applied to induce CT of the PIs as shown in the molecular simulation, the generated holes will delocalize to the porphyrin moieties thus result in an open channel for charge carrier migration. In addition, owing to zinc is chelated in the center of porphyrin units,

consequently, another possible route might be occurred from ITO (negative sweep) or Al (positive sweep) through metal zinc to porphyrin rings, resulting in ON state due to current increasing abruptly.

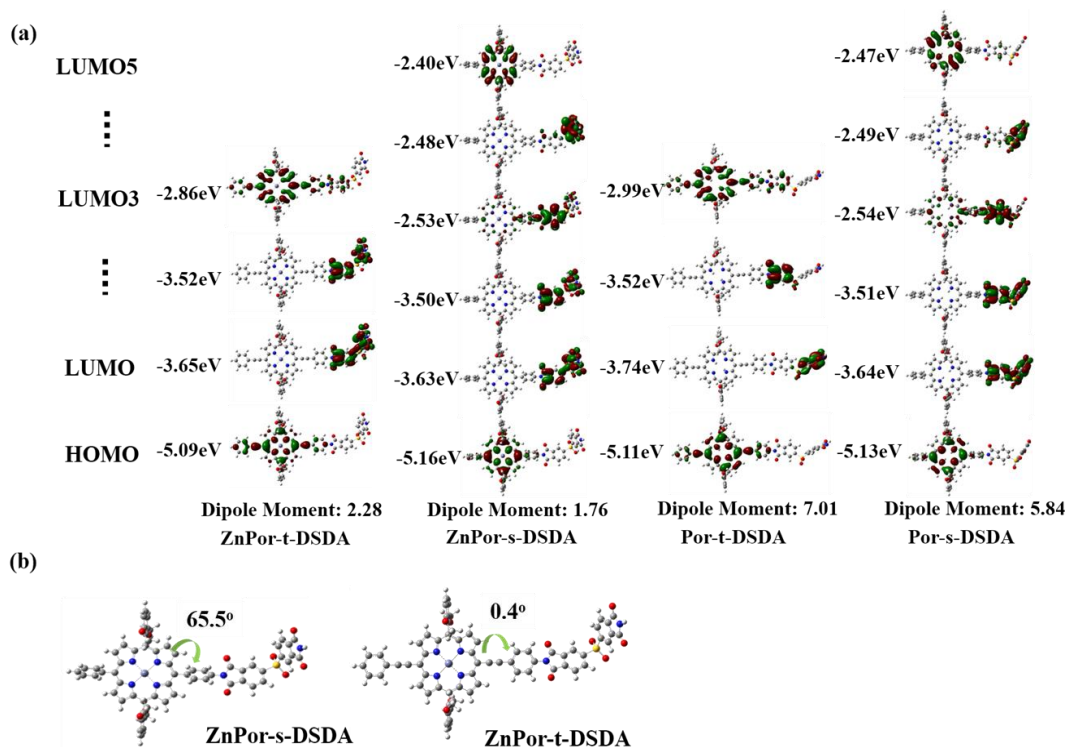


**Figure 6.** (a) Molecular simulation of the corresponding energy levels and (b) different linkages twist angle for the basic units of porphyrin-containing polyimide.

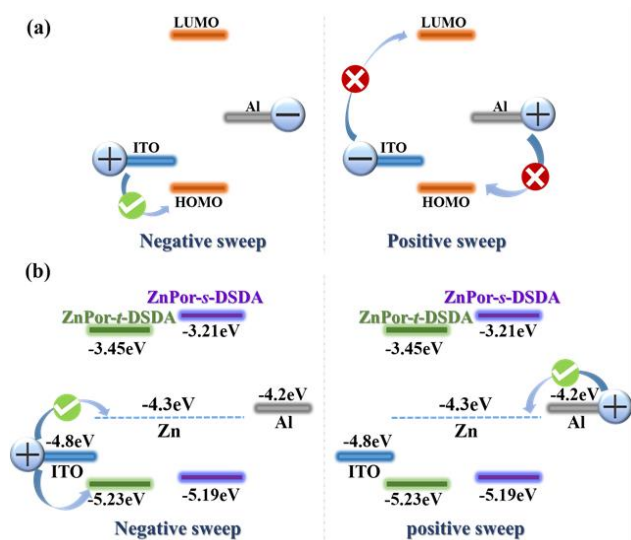


**Figure 7.** (a) Band diagram for general polyimide memory devices and (b) ITO/Zinc porphyrin-containing polyimide/Al.

## Conclusions

Three novel porphyrin-containing polyimides, **ZnPor-s-DSDA**, **Por-s-DSDA**, and **Por-t-DSDA**, were successfully prepared for

memory device application. The **ZnPor-s-DSDA** and **ZnPor-t-DSDA** exhibit WORM (>3hr) and DRAM (30s), respectively, ascribed to the linkage effect; the linkage resulting in non-coplanar PI structure could increase the retention time effectively. It is noteworthy of the interesting zinc effect on the memory behavior; only devices derived from these Zn-containing PIs (**ZnPor-s-DSDA** and **ZnPor-t-DSDA**) display memory properties. While, the **Por-s-DSDA** and **Por-t-DSDA** based devices behave no memory characteristic, demonstrating the significance of existing of metal zinc, which is the triggering for memory properties. Further understanding about the working mechanism and different metals (work function effect) of the metal-chelating porphyrin-containing polymers in memory application is very important and in progress.

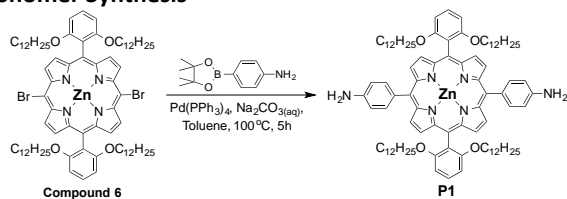
## EXPERIMENTAL

### Materials

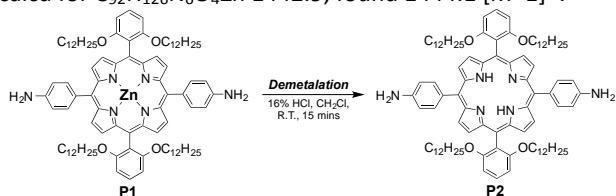
Air-sensitive materials were manipulated in glove box (MBraun Unilab). In addition, air-sensitive solutions were processed with vacuum Schlenk lines. **P3** was synthesized according to our previous report.<sup>17</sup> [5,15-Dibromo-10,20-bis(2,6-dioctoxyphenyl)porphyrinato] zinc(II) (**compound 6**) was synthesized according to the modified literature

conditions<sup>19</sup> and the detailed synthetic procedure and characterization of the precursors (**compound 2 to 6**) are referred to ESI. Commercially available 3,3',4,4'-diphenylsulfone tetracarboxylic dianhydride (DSDA) is purchased from TCI and purified by sublimation. Tetrabutylammonium perchlorate (TBAP) (ACROS) was purified by recrystallization from ethyl acetate under a nitrogen atmosphere and then dried *in vacuo* prior to use. All other commercially available reagents were used as purchased.

### Monomer Synthesis

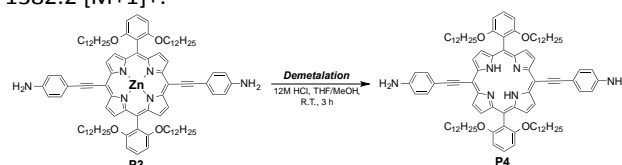


**P1:** To a solution, 2.5 g (1.73 mmol) of **compound 6** in 150 mL three-necked round bottom flask was added 40 mL of toluene and 0.39 g (0.34 mmol) of tetrakis(triphenylphosphine)palladium and the mixture was stirred at room temperature for 30 min. To this solution was added 5 mL of 2 M aqueous sodium carbonate followed by 1.48 g (6.92 mmol) of 4-(4,4,5,5-tetramethyl-1,3,2-dioxaborolan-2-yl)aniline (Aldrich) in 10 mL of ethanol. The resulting mixture was heated at reflux until no remained starting material detected by thin layer chromatography (TLC). Reaction mixture was filtered through diatomaceous earth, washed with ethyl acetate and subjected to column chromatography (silica gel) (dichloromethane/methanol = 9.8/0.2) followed by recrystallization to give 2.45 g of **P1** (97.22 % in yield). <sup>1</sup>H NMR (400 MHz, CDCl<sub>3</sub>): δ 8.87 (dd *J* = 4.4 Hz 4H), 8.83 (dd *J* = 4.4 Hz 4H), 7.91 (dd *J* = 2 Hz 4H), 7.67 (t *J* = 8.4 Hz 2H), 6.98 (d *J* = 8.4 Hz 2H), 6.76 (d *J* = 8 Hz 2H), 3.80 (t *J* = 6.4 Hz 8H), 3.11 (b, s NH, 4H), 1.53-0.365 (br, m 92H). <sup>13</sup>C NMR (100 MHz, CDCl<sub>3</sub>): δ 160.35, 150.52, 150.33, 144.55, 135.53, 134.39, 131.70, 130.92, 129.59, 122.44, 122.44, 119.81, 114.97, 113.49, 112.93, 105.67, 68.93, 32.02, 31.08, 21.62, 29.47, 29.40, 29.21, 28.88, 28.81, 25.35, 22.82, 14.25. Elemental analysis for C<sub>92</sub>H<sub>110</sub>N<sub>6</sub>O<sub>4</sub>Zn: calcd C: 74.37, H: 11.26, N: 5.66; found C: 75.95, H: 9.16, N: 5.55. FAB-MS: *m/z* calcd for C<sub>92</sub>H<sub>126</sub>N<sub>6</sub>O<sub>4</sub>Zn 1442.9, found 1444.1 [M+1]<sup>+</sup>.



**P2:** **P1** (1.0 g, 0.69 mmol) was taken in 100 mL of dichloromethane at room temperature added 16 % HCl (25 mL) stirred for 15 minutes. TLC showed complete absence of compound 8. PH adjusted to 7.5 by using saturated NaHCO<sub>3</sub> and extracted with dichloromethane. Organic layer was dried over MgSO<sub>4</sub> followed by removal of solvent under reduced pressure. Recrystallization by using dichloromethane/methanol gave 0.94 g of **P2** (98.9 % in

yield). <sup>1</sup>H NMR (400 MHz, CDCl<sub>3</sub>): δ 8.82 (d *J* = 4.8 Hz 4H), 8.77 (d *J* = 4.4 Hz, 4H), 7.99 (d *J* = 8.8 Hz, 4H), 7.69 (t *J* = 8.8 Hz, 2H), 7.04 (d *J* = 78.8 Hz, 4H), 6.99 (d *J* = 8 Hz, 4H), 3.97 (b, NH<sub>2</sub>, 4H), 3.81 (t, *J* = 6.4 Hz, 8H), 1.26-0.061 (br, m 92H). -2.61 (s, 2H). <sup>13</sup>C NMR (100 MHz, CDCl<sub>3</sub>): δ 160.43, 145.84, 135.84, 133.40, 129.94, 129.75, 131.70, 121.52, 119.01, 113.57, 112.44, 105.52, 32.08, 29.71, 29.57, 29.49, 29.47, 29.30, 28.97, 28.84, 25.51, 22.87, 14.31, 1.26. Elemental analysis for C<sub>92</sub>H<sub>128</sub>N<sub>6</sub>O<sub>4</sub>: calcd C: 77.68, H: 11.91 N: 5.91; found C: 79.35, H: 9.88, N: 5.77. FAB-MS: *m/z* calcd for C<sub>92</sub>H<sub>128</sub>N<sub>6</sub>O<sub>4</sub> 1381.0, found 1382.2 [M+1]<sup>+</sup>.



**P4:** 200 mg (0.134 mmol) of the **P3**<sup>17</sup> was dissolved in 80 mL of THF and 20 mL of methanol. After 10 mL of 12 M HCl(aq) was added, the mixture was then stirred at room temperature for 3 h. The reaction was monitored by TLC until the disappearance of starting material. Upon completion, 100 mL of Na<sub>2</sub>CO<sub>3</sub>(aq) was added slowly. The solvent was rotary evaporated and the residue was dissolved in dichloromethane again. After washed by NH<sub>4</sub>Cl (aq) and dried over Na<sub>2</sub>SO<sub>4</sub>, the solvent was rotary evaporated. The residue was then purified by column chromatography (silica gel) using EA/hexanes = 1/3 as eluent, followed by crystallization from dichloromethane/methanol to give 137.2 mg of **P4** (dark green solid, 71.7 % in yield). <sup>1</sup>H-NMR (300 MHz, CDCl<sub>3</sub>): δ 9.53 (d, *J* = 4.7 Hz, 4H), 8.72 (d, *J* = 4.6 Hz, 4 H), 7.78 (d, *J* = 8.3 Hz, 4H), 7.69 (t, *J* = 8.4 Hz, 2H), 6.98 (d, *J* = 8.4 Hz, 4H), 6.81 (d, *J* = 8.3 Hz, 4H), 3.92 (s, 4 H), 3.83 (t, *J* = 6.5 Hz, 8H), 1.27-0.75 (m, overlapped, 58H), 0.75-0.27 (m, overlapped, 32H), -1.78 (s, 2H). Elemental Anal for C<sub>96</sub>H<sub>128</sub>N<sub>6</sub>O<sub>4</sub> · 0.5H<sub>2</sub>O: calcd C 80.12 %, H 9.04 %, N 5.84 %; Found: C 80.03 %, H 8.96 %, N 5.82 %. MALDI-TOF: *m/z* calcd for C<sub>96</sub>H<sub>128</sub>N<sub>6</sub>O<sub>4</sub> 1429.0; found 1429.8 [M+H]<sup>+</sup>.

### Polyimide Synthesis

By using **ZnPor-t-DSDA** as an instance: by stirring the mixture of 0.224 g (0.15 mmol) of **P3** in 1.6 mL of *N,N*-dimethylacetamide (DMAc), 0.054 g (0.15 mmol) of DSDA at room temperature for 16 hours, and then the viscous poly(amic acid) can be obtained. The as-prepared poly(amic acid) was then directly converted to PI **ZnPor-t-DSDA** via chemical imidization method in the presence of acetic anhydride (0.6 mL) and pyridine (0.4 mL). After the reaction was processed at 120 °C for 4 h, the resulting PI solution was then poured into 300 mL of stirred methanol giving a fibrous precipitate, which was washed thoroughly with methanol and collected by filtration.

### Acknowledgements

The authors are grateful acknowledge to the Ministry of Science and Technology of Taiwan for the financial support.

## Notes and references

- 1 (a) W. L. Ma, C. Y. Yang, X. Gong, K. Lee, A. J. Heeger. *Adv. Funct. Mater.* 2005, **15**, 1617; (b) S. Gunes, H. Neugebauer, N. S. Sariciftci. *Chem. Rev.* 2007, **107**, 1324; (c) Y. J. Cheng, S. H. Yang, C. S. Hsu. *Chem. Rev.* 2009, **109**, 5868.
- 2 (a) F. Garnier, R. Hajlaoui, A. Yassar, P. Srivastava. *Science* 1994, **265**, 1684; (b) H. Yan, Z. H. Chen, Y. Zheng, C. Newman, J. R. Quinn, F. Dotz, M. Kastler, A. Facchetti. *Nature* 2009, **457**, 679.
- 3 (a) J. H. Burroughes, D. D. C. Bradley, A. R. Brown, R. N. Marks, K. Mackay, R. H. Friend, P. L. Burn, A. B. Holmes. *Nature* 1990, **347**, 539; (b) R. H. Friend, R. W. Gymer, A. B. Holmes, J. H. Burroughes, R. N. Marks, C. Taliani, D. D. C. Bradley, D. A. Dos Santos, J. L. Bredas, M. Lögdlund, W. R. Salaneck. *Nature* 1999, **397**, 121.
- 4 (a) H.-J. Yen, C.-J. Chen, G.-S. Liou. *Adv. Funct. Mater.* 2013, **23**, 5307; (b) Y. W. Chuang, H. J., Yen, J. H. Wu, G. S. Liou. *ACS Appl Mater Interfaces* 2014, **6**, 3594; (c) J.-H. Wu, G.-S. Liou. *Adv. Funct. Mater.* 2014, **24**, 6422.
- 5 (a) J. H. Wu, G. S. Liou. *ACS Appl Mater Interfaces* 2015, **7**, 15988; (b) H.-J. Yen, C.-J. Chen, J.-H. Wu, G.-S. Liou. *Polym. Chem.* 2015, **6**, 7464.
- 6 P. O. Sliva, G. Dir, C. Griffiths. *J. Non-Cryst. Solids.* 1970, **2**, 316.
- 7 W. P. Lin, S. J. Liu, T. Gong, Q. Zhao, W. Huang. *Adv. Mater.* 2014, **26**, 570.
- 8 (a) H. C. Wu, C. L. Liu, W. C. Chen. *Polym. Chem.* 2013, **4**, 5261; (b) H. J. Yen, H. Tsai, C. Y. Kuo, W. Nie, A. D. Mohite, G. Gupta, J. Wang, J. H. Wu, G. S. Liou, H. L. Wang. *J. Mater. Chem. C* 2014, **2**, 4374; (c) W. Elsaywy, M. Son, J. Jang, M. J. Kim, Y. Ji, T. W. Kim, H. C. Ko, A. Elbarbary, M. H. Ham, J. S. Lee. *ACS Macro Letters* 2015, **4**, 322.
- 9 (a) S. L. Lim, Qidan, E. Y. H. Teo, C. X. Zhu, D. S. H. Chan, E. T. Kang, K. G. Neoh. *Chem. Mater.* 2007, **19**, 5148; (b) S. G. Hahm; N. G. Kang, W. Kwon, K. Kim, Y. G. Ko, S. Ahn, B. G. Kang, T. Chang, J. S. Lee, M. Ree. *Adv. Mater.* 2012, **24**, 1062; (c) S. J. Liu, P. Wang, Q. Zhao, H. Y. Yang, J. Wong, H. B. Sun, X. C. Dong, W. P. Lin, W. Huang. *Adv. Mater.* 2012, **24**, 2901; (d) S. Miao, Y. Zhu, H. Zhuang, X. Xu, H. Li, R. Sun, N. Li, S. Ji, J. Lu. *J. Mater. Chem. C* 2013, **1**, 2320.
- 10 (a) L. C. Lin, H. J. Yen, C. J. Chen, C. L. Tsai, G. S. Liou. *Chem. Commun.* 2014, **50**, 13917; (b) J. H. Wu, H. J. Yen, Y. C. Hu, G. S. Liou. *Chem. Commun.* 2014, **50**, 4915.
- 11 (a) A. D. Yu, C. L. Liu, W. C. Chen. *Chem. Commun.* 2012, **48**, 383; (b) M. A. Khan, U. S. Bhansali, D. Cha, H. N. Alshareef. *Adv. Funct. Mater.* 2013, **23**, 2145; (c) C. L. Tsai, C. J. Chen, P. H. Wang, J. J. Lin, G. S. Liou. *Polym. Chem.* 2013, **4**, 4570; (d) C. J. Chen, J. H. Wu, G. S. Liou. *Chem. Commun.* 2014, **50**, 4335.
- 12 Q. D. Ling, F. C. Chang, Y. Song, C. X. Zhu, D. J. Liaw, D. S. Chan, E. T. Kang, K. G. Neoh. *J. Am. Chem. Soc.* 2006, **128**, 8732.
- 13 H.-J. Yen, G.-S. Liou. *Polym. J.* 2016, **48**, 117.
- 14 (a) A. Yella, H. W. Lee, H. N. Tsao, C. Yi, A. K. Chandiran, M. K. Nazeeruddin, E. W. Diau, C. Y. Yeh, S. M. Zakeeruddin, M. Gratzel. *Science* 2011, **334**, 629; (b) C.-L. Wang, M. Zhang, Y.-H. Hsiao, C.-K. Tseng, C.-L. Liu, M. Xu, P. Wang, C.-Y. Lin. *Energy Environ. Sci.* 2016, **9**, 200.
- 15 (a) C. T. Chen. *Chem. Mater.* 2004, **16**, 4389; (b) B. S. Li, J. Li, Y. Q. Fu, Z. S. Bo. *J. Am. Chem. Soc.* 2004, **126**, 3430.
- 16 (a) Y. Y. Noh, J. J. Kim, Y. Yoshida, K. Yase. *Adv. Mater.* 2003, **15**, 699; (b) X. B. Huang, C. L. Zhu, S. M. Zhang, W. W. Li, Y. L. Guo, X. W. Zhan, Y. Q. Liu, Z. Z. Bo. *Macromolecules* 2008, **41**, 6895.
- 17 M.-C. Tsai, C.-L. Wang, C.-Y. Lin, C.-L. Tsai, H.-J. Yen, H.-C. You, G.-S. Liou. *Polym. Chem.* 2016, **7**, 2780.
- 18 (a) T.-T. Huang, C.-L. Tsai, S.-H. Hsiao and G.-S. Liou. *RSC Adv.*, 2016, **6**, 28815; (b) C.-J. Chen, H.-J. Yen, Y.-C. Hu, G.-S. Liou. *J. Mater. Chem. C* 2013, **1**, 7623; (c) C. J. Chen, Y. C. Hu, G. S. Liou. *Chem. Commun.* 2013, **49**, 2536; (d) Y.-H. Chou, H.-J. Yen, C.-L. Tsai, W.-Y. Lee, G.-S. Liou, W.-C. Chen. *J. Mater. Chem. C* 2013, **1**, 3235.
- 19 (a) C. Y. Lee, J. T. Hupp, *Langmuir* 2010, **26**, 3760; (b) A. Yella, H. W. Lee, H. N. Tsao, C. Yi, A. K. Chandiran, M. K. Nazeeruddin, E. W. Diau, C. Y. Yeh, S. M. Zakeeruddin, M. Gratzel, *Science* 2011, **334**, 629.
- 20 (a) C.-J. Chen, Y.-C. Hu, G.-S. Liou. *Polym. Chem.* 2013, **4**, 4162; (b) H.-J. Yen, J.-H. Chang, J.-H. Wu, G.-S. Liou. *Polym. Chem.* 2015, **6**, 7758.
- 21 C.-J. Chen, C.-L. Tsai, G.-S. Liou. *J. Mater. Chem. C* 2014, **2**, 2842.

## The table of contents entry

View Article Online  
DOI: 10.1039/C6RA18986E

## Zinc and linkage effects of novel porphyrin-containing polyimides on resistor memory behaviors

Chia-Liang Tsai,<sup>a,†</sup> Kamani Sudhir K Reddy,<sup>b,†</sup> Chen-Yu Yeh,<sup>b,\*</sup> Chin-Li Wang,<sup>c</sup> Ching-Yao Lin,<sup>c,\*</sup> Hung-Ju Yen,<sup>a</sup> Ming-Chi Tsai<sup>a</sup> and Guey-Sheng Liou<sup>a,\*</sup>

A series of porphyrin-containing polyimides were synthesized for resistor type memory application. The retention time of memory devices could be tuned by the linkage groups between porphyrin moiety (donor) and DSDA (acceptor). Moreover, the metal zinc also plays an important role in further tuning the memory behavior.

